Available online at www.sciencedirect.com

SciVerse ScienceDirect

Ceramics International 38 (2012) 1663–1670

CERAMICS INTERNATIONAL

www.elsevier.com/locate/ceramint

Photoluminescence and microstructural properties of SiO_2–ZnO–B_2O_3 system containing TiO_2 and V_2O_5

Shamsi Sadat Alavi Qazvini [a], Zohreh Hamnabard [b,*], Zahra Khalkhali [c], Saeid Baghshahi [d], Amir Maghsoudipour [e]

[a] Department of Materials Enginneering, Science and Research Branch, Slamic Azad University, Tehran, Iran
[b] Material Research School, P.O. Box 14395-836, Alborz, Iran
[c] Department of Material Science, Ceramic Division, Iran University of Science and Technology, Tehran, Iran
[d] Faculty of Engineering and Technology, I.K.I. University, Qazvin, Iran
[e] Department of Ceramics, Materials and Energy Research Center, Alborz, Iran

Received 12 June 2011; received in revised form 20 September 2011; accepted 28 September 2011
Available online 23 October 2011

Abstract

Phase analysis, thermal behavior, microstructure and photoluminescence properties of six specimens in a ZnO–SiO_2–B_2O_3 ternary glass system were investigated by means of DTA, XRD, SEM and PL spectroscopy to reveal the effect of introducing different TiO_2 and V_2O_5 contents to the base glass composition. Both chemicals improved crystallization through reducing the surface energy as well as disrupting the large scale order in the glass network. The optical basicity of every individual metal oxide included in the samples was presented as an estimation of the number of non bridging oxygens (NBOs). Facilitated precipitation of willemite and ZnO due to introducing TiO_2 and V_2O_5 to the base glass compensated for the increase of NBOs and ultimately resulted in the enhancement of width and intensity of the near band edge emission.

Keywords: B. Spectroscopy; C. Optical properties; D. TiO_2, D. ZnO

1. Introduction

As an important ceramic material as well as a wide band gap donor semiconductor (3.37 eV at room temperature), zinc oxide (ZnO) has found many technological applications in gas sensors, catalysts, solar cells, etc. [1–4]. Recently, its optical applicability for instance in gamma ray detectors and vacuum fluorescent displays (VFD's) has attracted numerous research interests [5]. ZnO contains two luminescence bands:

1. A relatively thin band of about 3.25 ev intensity on the UV-region at approx 380 nm.
2. A relatively wide band on the visible region (500–600 nm) with the intensity of about 2.35–2.5 ev.

Near-band-edge (NBE) emission due to the recombination of electrons and holes leads to the UV-emission [2,6] and the transition of trapped electrons due to intrinsic defects such as oxygen vacancies (V_O), oxygen interstitials (O_{in}) and zinc interstitials (Zn_{in}) causes the visible emission [2,7].

ZnO visible emission lifetime is in the μs range while that of the ultraviolet emission is of the order of several tens to hundreds of picoseconds [5] and thereby makes ZnO appropriate for superfast scintillators [8]. Glass–ceramics have high physical and chemical stability and are fabricated easily. Meanwhile, they comprise the advantages of both glasses and single crystals at the same time. Furthermore, ZnO eliminate grain boundaries in the glass network and leads to an enhancement in the luminescence properties [9]. Therefore, ZnO containing glass ceramics have become important alternatives to crystal detectors [2–10]. Crystallization, grain size and distribution of ZnO particles in the glass matrix which characterize the Photoluminescence (PL) spectrum of the glass over the UV and visible region are affected significantly by the

* Corresponding author. Tel.: +98 2614464088; fax: +98 2614464097.
E-mail addresses: zhamnabard@nrcam.org (Z. Hamnabard), IRUH81@yahoo.com (S.S.A. Qazvini), khalkhali_z@yahoo.com (Z. Khalkhali), s.baghshahi@ikiu.ac.ir (S. Baghshahi), a_maghsoudi@merc.ac.ir (A. Maghsoudipour).

0272-8842/$36.00
doi:10.1016/j.ceramint.2011.09.058

glass composition. So far various dopants have been introduced to ZnO-based scintillating glasses to improve their PL properties. (e.g. Ti^{4+} and Ce^{2+} to enhance irradiation resistance [11], Eu^{3+} and V^{4+} to produce red-emitting phosphors [12], etc.). However, a few articles focused on the effect of different dopants on the emission wavelength and intensity of near-band-edge (NBE) spectra of ZnO-based glasses. TiO_2 and V_2O_5 are both highly polarizable and render glasses semiconductive. The objective of this work is to investigate the effect of introducing different TiO_2 and V_2O_5 contents to a $ZnO–SiO_2–B_2O_3$ ternary glass system on thermal, microstructural and photoluminescence properties in order to develop scintillating ZnO-based glasses with a high PL efficiency.

2. Materials and methods

Glass specimens were prepared using melt quenching method with compositions listed in Table 1. G is the base glass composition. 1, 2 and 3 mole V_2O_5 was added to the base glass and formed GV1, GV2, GV3. Similarly, 2 and 3 mole TiO_2 was introduced to G to produce GTi2 and GTi3, respectively. Standard reagent grade SiO_2, H_3BO_3, ZnO, TiO_2 powders were chosen as the starting materials. The 100-g batches of each six sample were melted in a high alumina crucible in an electric furnace at 1400 °C for 3 h in air. The melt was poured into a preheated steel mould and was annealed at about 600 °C for 2 h to release the internal stresses formed during quenching. Then the furnace was turned off until specimens were cooled down to room temperature. Differential thermal analysis was run on powdered glass specimens with the particle size of (45 μm≥) and (225 μm≤) by means of a STA apparatus (1500-Rheometric scientific) at the heating rate of 10 °C/min. Cubic specimens were cut out of the glass and were heat treated at exothermic peak temperatures for 3 h. Crystalline phases were investigated by X-ray diffractometry (Philips-PW1800) with Cu K_α radiation and scanning from 5° to 75°. Polished surface of the glass specimens were etched in 10 vol. % HF solutions for 5–20 s and analyzed by scanning electron microscopy (PHILIPS-XL30). Glass specimens were powdered to 225 μm≤ particle size and underwent photoluminescence spectra measurements over the UV and visible region (250–550 nm) by means of a fluorescence spectrophotometer (Perkin–Elmer LS-5) using excitation light at different wavelengths at room temperature in air.

Table 1
Composition and optical basicity of the glass samples (part by mole).

	ZnO	SiO_2	B_2O_3	V_2O_5	TiO_2	$\Lambda_{th} \pm 0.001$
G	60	25	15	–	–	0.501
GV1	60	25	15	1	–	0.503
GV2	60	25	15	2	–	0.504
GV3	60	25	15	3	–	0.506
GTi2	60	25	15	–	2	0.502
GTi3	60	25	15	–	3	0.503

3. Results

Fig. 1 presents DTA analysis of the glass specimens. The glass transition temperature T_g decreased gradually from 595 °C to 572 °C upon gradual increment of V_2O_5 or TiO_2 from 0 to 3 mole. Glass transition is the reversible transition in amorphous materials from a hard and relatively brittle state into a molten or rubber-like state. The transition induces a smooth increase in the viscosity of a material upon cooling. Contrary to viscosity, the thermal expansion, heat capacity, and many other properties of glasses show a relatively sudden change at the glass transition temperature.

A main exothermic peak appeared on the DTA thermogram of G which with increasing V_2O_5 from 0 to 3 moles shifted down slightly from 775 °C to 772 °C. However, no change occurred in the sharpness of the peak. Similarly, introducing TiO_2 to the base glass shifted the exothermic peak from 775 °C to a lower temperature (768 °C) without any changes in the sharpness of the peak. GTi3 was the only specimen with two exothermic peaks appeared at 768 °C and 780 °C, respectively. It is worth mentioning that the shoulder of the exothermic peak seen in the other samples' thermograms have been formed because of melting of the samples at around 900 °C and thus we did not consider the shoulders as exothermic peaks.

DTA analysis was run on both fine (45 μm≥) and coarse (225 μm≤) particle size of the base glass composition G in order to determine the effect of particle size on thermal behavior of the glass. The result is presented in Fig. 2. It is seen that the peak crystallization temperature is shifted up from 775 °C to 840 °C and meanwhile increased noticeably in intensity upon replacing the fine particles by the coarse ones. Therefore, it seems reasonable to conclude that the main crystallization mechanism in the present system is by the surface rather than bulk.

According to the X-ray diffraction patterns of the samples after annealing at 600 °C for 2 h (Fig. 3) all samples were amorphous and crystal free prior to heat treatment. Fig. 4 indicates XRD patterns of the samples after a 3 h heat treatment

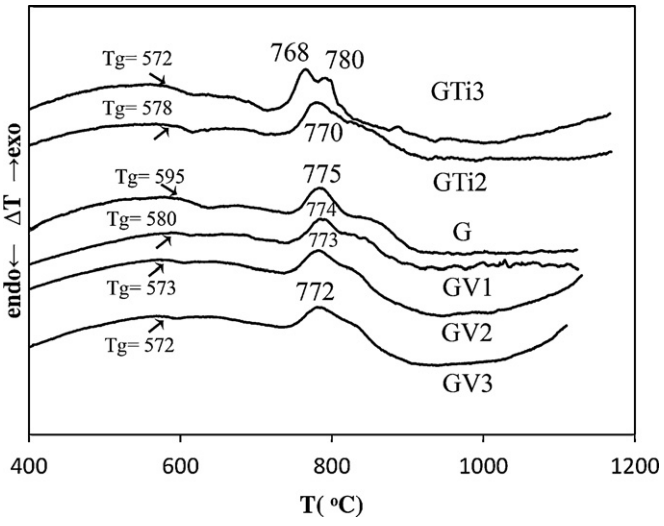

Fig. 1. DTA curves of the glass specimens.

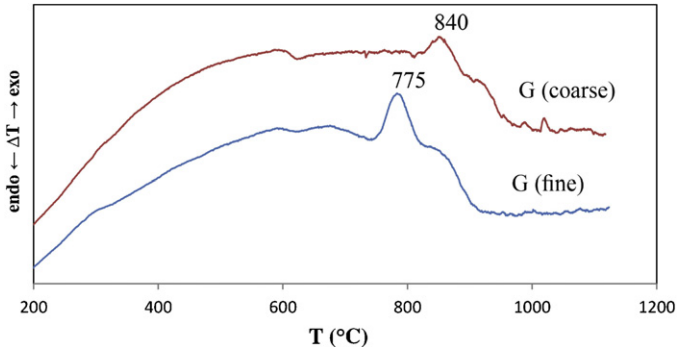

Fig. 2. DTA thermograms of fine and coarse particle size of the base glass G.

at their peak exothermic temperatures. From this figure it is obvious that ZnO is the only crystalline phase precipitated in the base glass. Doping of the base glass with different amounts of Ti^{4+} and V^{5+} significantly affected the amount and kind of the crystalline phases formed within the glass. Increasing the amount of V_2O_5 from 0 to 3 moles resulted in the precipitation of vanadium oxide (VO_2) and willemite (Zn_2SiO_4) which increased in the intensity by the dopant content. Again according to Fig. 4, it is seen that with introducing 2 mole TiO_2 to G, XRD peaks of ZnO crystals sharpened noticeably at the exothermic peak of GTi2, whereas 3 mole TiO_2 decreased the intensity of ZnO crystals at the first exothermic peak temperature (768 °C) and induced willemite crystals to precipitate at the second exothermic peak temperature (780 °C). In a view of above-discussed data, it seems clear that the mere exothermic peak emerged in the thermograms of G and GTi2 is attributed to the crystallization of ZnO while that of GV1, GV2 and GV3 is assigned to precipitation of willemite and vanadium oxide crystals. Thus, the presence of three crystallization peaks overlapping with each other has led to a wide exothermic peak in the thermograms of the three latter samples. Moreover, the two exothermic peaks in the GTi3 thermogram are representative of ZnO and willemite, respectively.

Fig. 5 presents micrographs of etched surfaces of the specimens heat treated at their peak crystallization temperatures for 3 h. As in most silicate glasses, the glass matrix

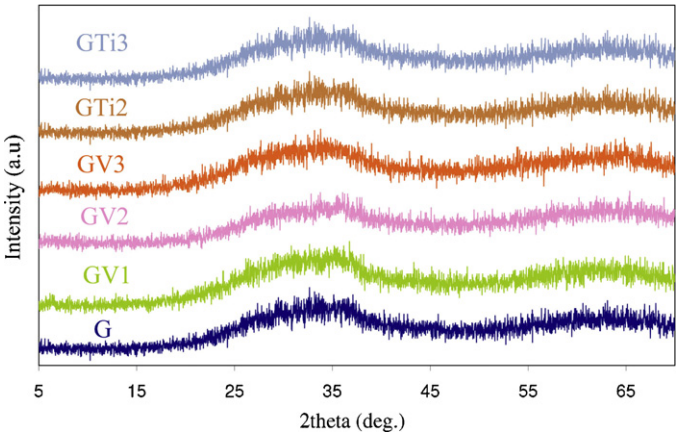

Fig. 3. XRD patterns of G, GV_3, GV_6 and GV_9 heat treated at their peak crystallization temperature (775 °C) for 3 h.

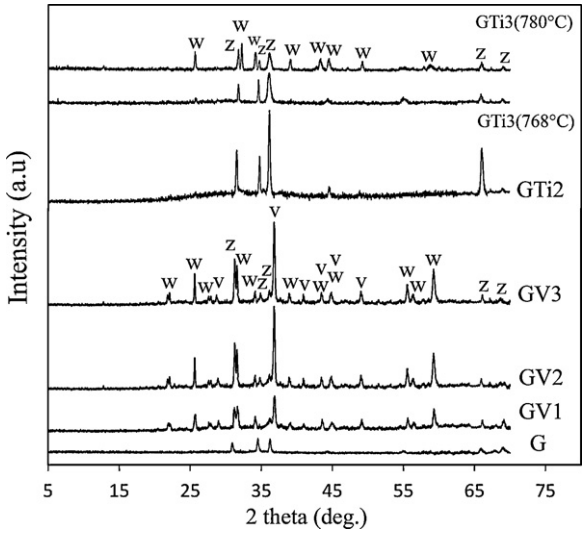

Fig. 4. XRD patterns of G, GTi_2 and GTi_4 heat treated at their peak crystallization temperatures for 3 h.

dissolves in HF acid more easily than the crystalline phases, we etched the polished surface of the samples prior to SEM analysis in order to make the precipitated phases more clear. It is seen from Fig. 5(a–d) that upon gradual increment of V_2O_5, some star-like crystals formed within the glass (in GV1) which decreased slightly in size but increased in concentration (in GV2 and GV3). Meanwhile, the crystal morphology changed from star to cubic aggregates. EDX analysis provided in Fig. 6 shows that they are willemite (Zn_2SiO_4) crystals which match the XRD results. Peaks of Au in the EDX pattern are due to the golden coat of the SEM samples. Fig. 5(e) shows that addition of 2 mole TiO_2 to the glass again led to the precipitation of star-like crystals. The morphology of the crystals remained unchanged upon addition of 2 or 3 mole TiO_2. Fig. 5(f, g) shows that with increasing the TiO_2 content from 2 to 3 moles, star-like crystals precipitated more intensively after a 3 h heat treatment at the first and second crystallization peak temperature. Fig. 7 presents the EDX analysis on the pointed aggregate in Fig. 5(g) which is rich of Zn^{2+} and Si^{4+} ions and confirms precipitation of willemite in these glasses. All star-like and cubic crystals tended to grow radially from a core which is probably the V^{5+} and Ti^{4+} ion in the V-doped and Ti-doped sample, respectively. Because the representative peaks of V and Ti emerged in the EDX analysis (Figs. 6 and 7). Another observation in the SEM micrographs is that Ti-doped glasses contain extremely finer crystals than V-doped ones.

Room temperature PL spectra of G, GV3 and GTi3 after heat treating at around nucleation temperature (610 °C) for 3 h and photoexciting at different wavelengths are presented in Figs. 8–10, respectively. Emission spectrum of ZnO particles is also included in the inset of Fig. 8 for comparison. A wide emission band over the visible region in ZnO particles is eliminated in the PL bands of G, GV3 and GTi3 and the NBE emission shifted to larger wavelengths with respect to that of ZnO particles. Meanwhile, the latter band engaged a larger wavelength range over the UV and extended to the violet region. This effect even was intensified as the base glass was doped with 3 mole V_2O_5 or

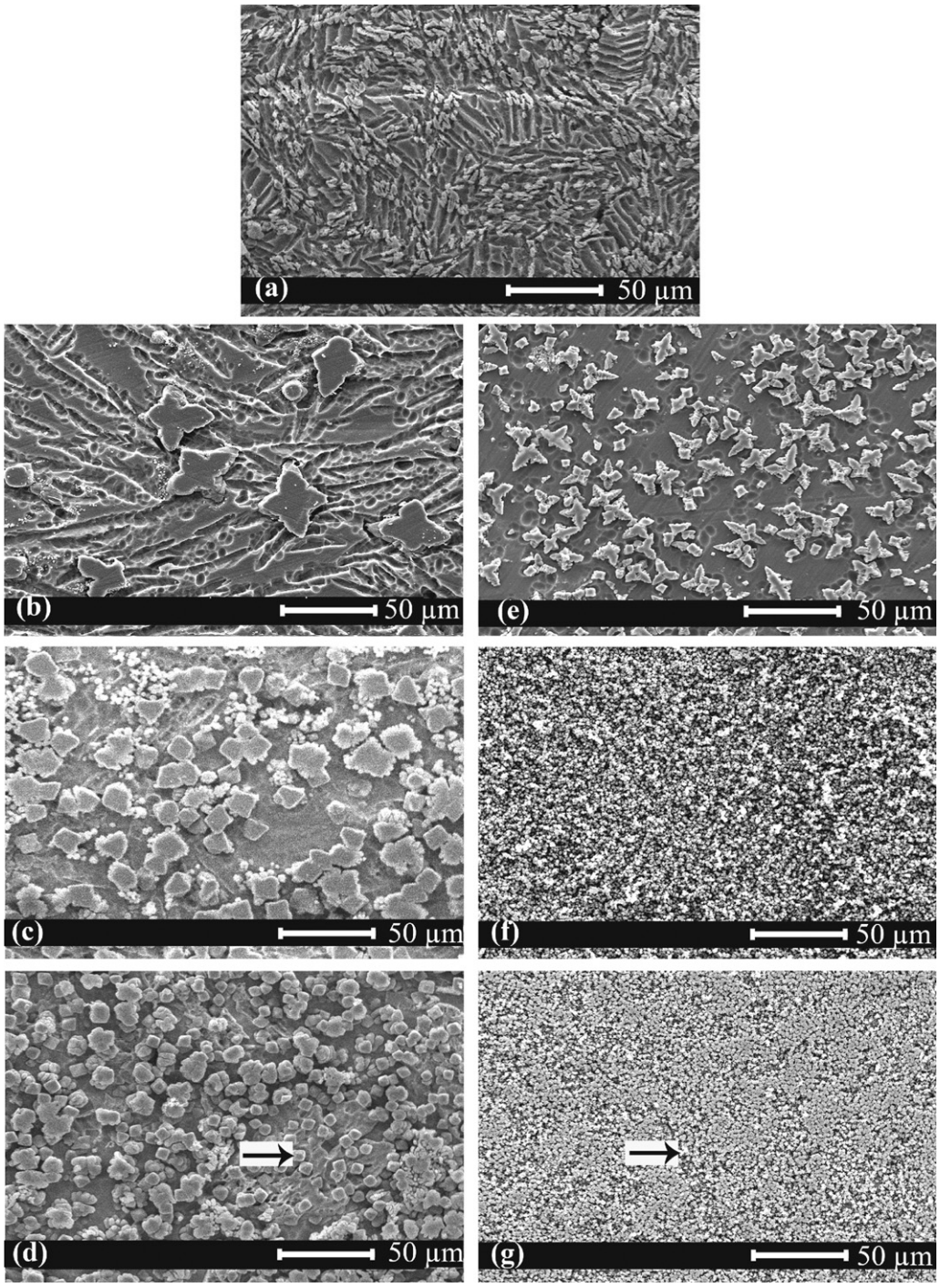

Fig. 5. Micrographs of (a) G, (b) GV1, (c) GV2 and (d) GV3 heat treated at 775 °C for 3 h and (e) GTi2 heat treated at 770 °C and GTi3 heat treated at (f) 768 °C and (g) 780 °C for 3 h.

TiO_2. Heat treating at nucleation temperature results in achieving ZnO nanoparticles which have larger ratios of surface to volume than coarse particles and thus can be excited more easily and will lead to a more intensive NBE emission [9,13,14]. The excitation wavelength for ZnO-based scintillating glasses is around 262 nm [14,15]. In the present study emission spectra of the specimens were measured at 262, 280, 290, 300 and 310 nm excitation wavelengths among which 280 nm was chosen as the optimum excitation wavelength for G and GV3 while 290 nm was chosen as the optimum excitation wavelength for GTi3 because a broad emission band peaked at a certain NBE wavelength is important for a desirable scintillator to achieve good timing resolution [16].

The emission band of GV3 peaked at 375, 425, 450, 462 and 490 nm at every studied excitation wavelength while a mere band peak of GTi3 attained at 450 nm after excitation at different wavelengths excluding λ_{exc} = 262 nm.

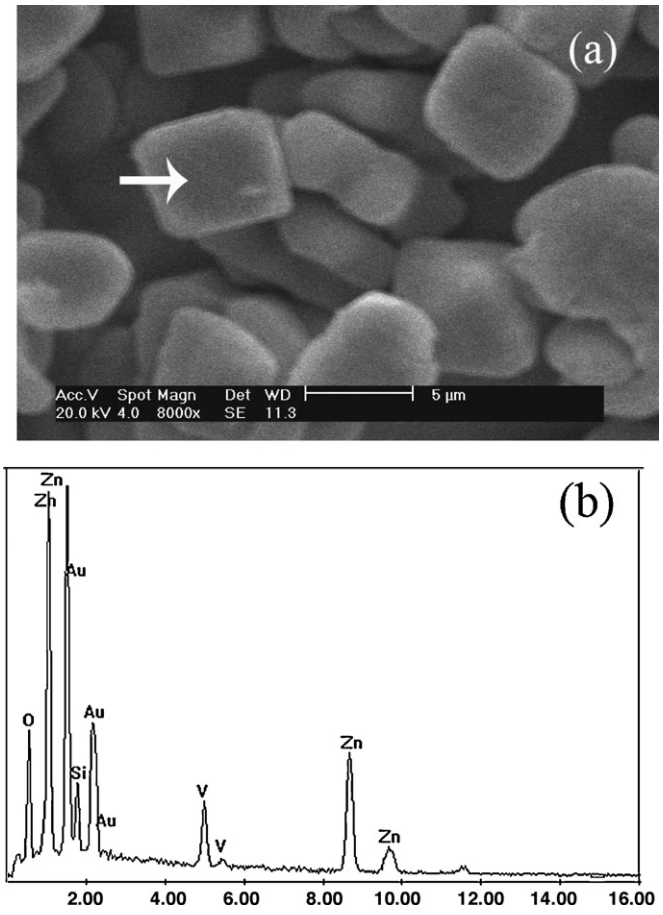

Fig. 6. (a) High magnification micrograph and (b) EDX analysis of the pointed aggregate in Fig. 5(d).

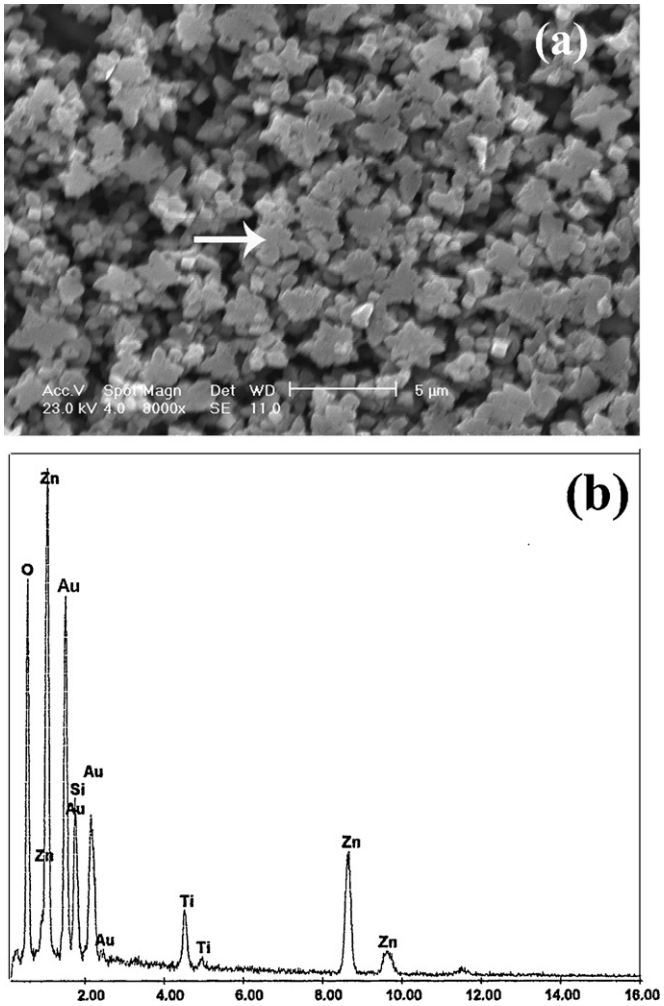

Fig. 7. (a) High magnification micrograph and (b) EDX analysis of the pointed aggregate in Fig. 5(g).

Fig. 11 compares photoluminescence spectra of G, GV3 and GTi3 excited at their optimum excitation wavelengths. Both dopants increased the peak intensity of the PL band. However, Ti-doped glass exhibited a smoother band than V-doped one.

4. Discussion

According to the DTA thermograms both V_2O_5 and TiO_2 reduced T_g and T_{cr} to lower temperatures with respect to those of G. this means that both additives reduced the viscosity of glass and meanwhile improved crystallization. There may be three origins for this effect: one is that the effective ionic radius of both Ti^{4+} (0.60 Å) and V^{5+} (0.54 Å) are larger than that of Si^{4+} (0.26 Å) [10] and thereby both dopants disrupted the large scale glass network leading to less viscosity of the glass as well as easier diffusion of ions to form crystals. The second contribution of these two chemicals to the reduction of viscosity and improvement of crystallization might be through the number of non-bridging oxygens which get larger with addition of both V_2O_5 and TiO_2 to the base glass regarding the theoretical optical basisity which is calculated for each sample.

The theoretical optical basicity Λ_c is a chemical parameter based on the ionic nature of oxides which provides an estimation of the number of (NBOs) and can be calculated through the following relation proposed by Duffy and Ingram [16] for a given metal oxide:

$$\Lambda_c = \frac{Z_c r_c}{2\gamma_c} \tag{1}$$

where Z_c is the oxidation number of the cation, r_c is the ratio of the number of cations to the number of oxides present and γ_c is the basicity moderating parameter. The basic moderating parameter can be estimated through Eq. (2).

$$\gamma_c = 1.36(x_m - 0.26) \tag{2}$$

where x_m is the electronegativity of the metal ion [17]. Table 2 lists the electronegativities of the metal ions, basicity moderating parameters and bulk optical basicities of individual metal oxides included in glass compositions. It is seen that the more x_m, the less the optical basicity. Λ_c decreases in the sequence of V_2O_5, TiO_2, ZnO, SiO_2 and B_2O_3. It is possible to calculate so-called theoretical optical basicity Λ_{th} of a glass through the following equation:

$$\Lambda_{th} = \sum x_c \Lambda_c \tag{3}$$

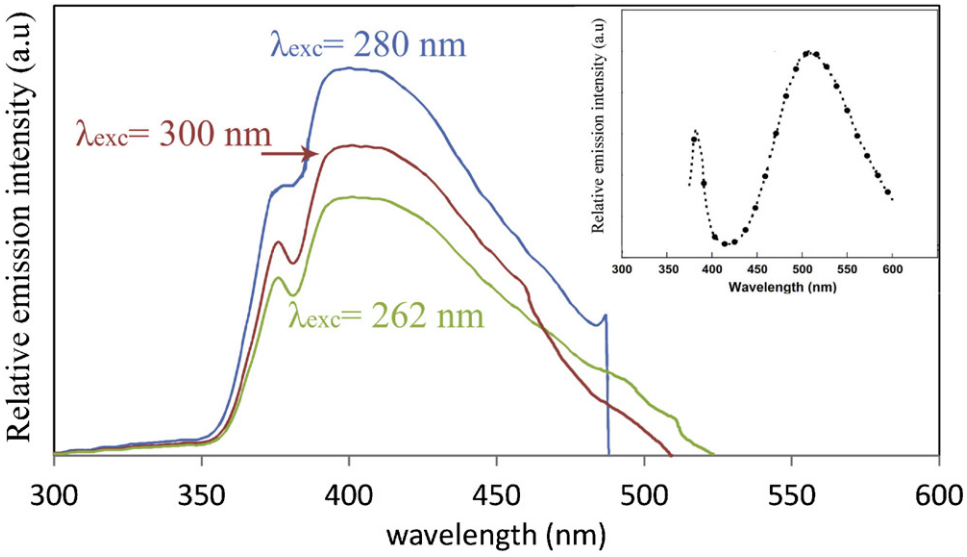

Fig. 8. Photoluminescence spectra of G excited at different wavelengths. The inset shows the PL spectrum of ZnO particles after excitation at 262 nm.

where x_c and Λ_c are the equivalent molar fraction and optical basicity of oxide c, respectively [18]. Λ_{th} of each glass is provided in Table 1. It can be seen that both additives increased the theoretical optical basicity and thus the number of NBOs. The more the NBOs, the more the tendency to form structural units of oxide atoms [18], which leads to a less viscosity and expectedly a more intense crystallization. Finally the third origin of the T_g and T_{cr} reduction upon the increment of V_2O_5 and TiO_2 is that these dopants reduce the surface tension [10] and convert the main crystallization mechanism from surface to bulk by producing heterogeneous nucleation sites and thereby reducing the surface energy of crystalline nuclei within the glass matrix. XRD and SEM analysis also supported the fact that TiO_2 and V_2O_5 acted as nucleating agents in this glass system since a more intense crystallization of willemite and ZnO occured in V and Ti- doped samples compared to that of the base glass.

Conclusively, intrinsic defects consisting of vacancies, interstitials, dislocations, etc. deteriorate the performance of a semiconductor scintillator. Such defects together with impurities act as nonradiative recombination centers and result in excitation energy lost [15]. Therefore the elimination of the wide emission band over the visible region in G, GV3 and GTi3 with respect to that of ZnO particles can be attributed to embedding ZnO particles in a glass matrix. From this point of view, introducing 3 mole V_2O_5 or TiO_2 to the base glass improves PL emission band as both UV and visible emission processes compete with each other and elimination of one process will strengthen the other.

SEM micrographs are evidence enough that willemite and ZnO crystals precipitated more intensively in V- and Ti-doped glasses with respect to those of the base glass. Meanwhile, the particle size of the crystals decreased significantly due to the nucleating agent role of both dopants. Therefore, photoluminescent constituents contained in GV3 and GTi3 required less excitation energy than those of G due to their larger ratio of surface to volume and ultimately enhanced the PL band intensity.

On the other hand, although the NBE band of G grew sharper upon introducing 3 mole V_2O_5 to the base glass (Fig. 8), different emission peaks emerged in the emitted band is not favorable for scintillating glasses [2,15]. The latter might be originated by the various valencies of vanadium when

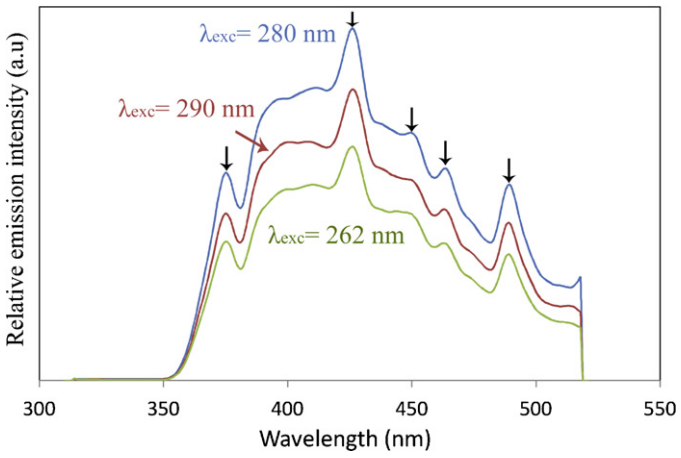

Fig. 9. Photoluminescence spectra of GV3 excited at different wavelengths.

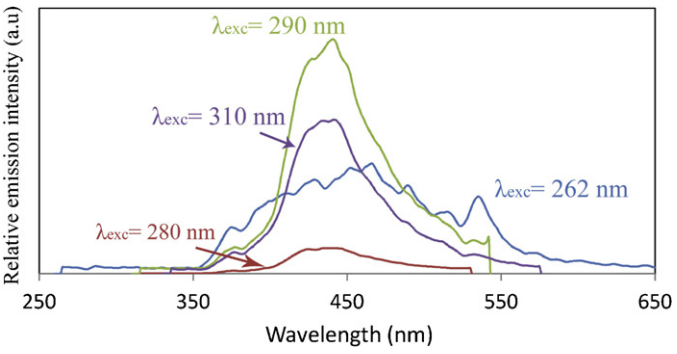

Fig. 10. Photoluminescence spectra of GTi3 excited at different wavelengths.

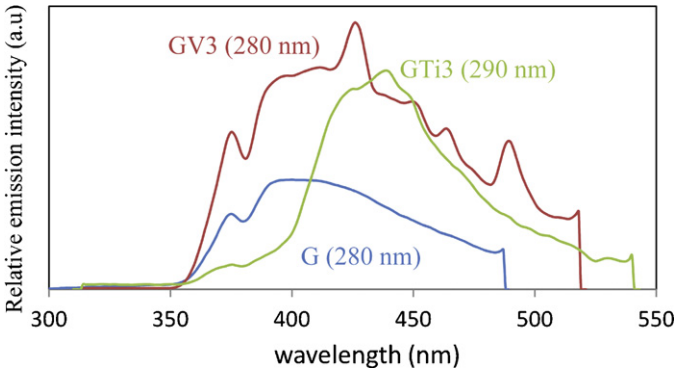

Fig. 11. Comparative photoluminescence spectra of G, GV3 and GTi3 excited at their optimum excitation wavelengths.

embedded in a glass matrix. Vanadium is a high polarizable ion with the atomic refractivity of R_a [V] = 25.6. In glass, vanadium occurs in several valencies consisting of pentavalent (V_2O_5), tetravalent (VO_2), trivalent (V_2O_3) and bivalent (VO) leading to various band peaks. Moreover, one other cause of this effect is reported by researchers to be network defects induced during glass preparation [2]. Tahir et al. [19] studied optical properties of V-doped ZnO nanoparticles and found that with increasing the vanadium content, the lattice parameters increased due to the incorporation of V into the ZnO lattice.

Almost similar to vanadium, titanium is a high polarizable ion with the atomic refractivity of R_a [Ti] = 19 and improves semiconductive properties including PL band by introducing acceptor levels in the band gap of the host matrix.

A detailed understanding of the optical bacisity [18] and compounds vibration properties within the glass network [20] is required to characterize PL spectroscopy. Furthermore, the mean free path of photons, the mass attenuation coefficient and the effective atomic number are basic parameters for determining the penetration of gamma-ray photons in a given material. UV-absorption of oxide glasses is predominantly due to excitation of electrons of oxygen ions and weakly bonded nonbridging oxygens (NBOs) are most prone to this effect [21]. Oxygen ion absorption in the UV–vis region increases in the following sequence: bridging oxygens between tetrahedral, nonbridging oxygens in $Si–O^-$ bonds and bridging oxygens stretched unsymmetrically within the tetrahedral [18]. The weaker is the bond, the more absorption occurs. From this point of view, the NBE emission of doped samples must have been decreased in sharpness with respect to that of the base glass G. In spite of this Fig. 11 shows that both dopants increased the sharpness and width of the UV emission band compared to that of G. Thereupon there must have been another factor that surpasses the effect of enlarging the number of NBOs as a result of doping the glass with V_2O_5 and TiO_2. Thus it seems reasonable that after heat treating the samples at 610 °C for 3 h willemit and ZnO precipitated in GV3 and GTi3 respectively, although below our XRD apparatus detection level. Moreover, as proved by SEM investigations precipitation of willemite which is a photoluminescent crystal has been facilitated with addition of V_2O_5 or TiO_2.

Table 2
Electronegativities of metal ions, basicity moderating parameters and bulk optical basicities of individual metal oxides included in glass compositions.

oxide	x_m	γ_m	Λ_c
SiO_2	1.8	2.08	0.48
B_2O_3	2	2.36	0.42
ZnO	1.65	1.87	0.53
TiO_2	1.6	1.82	0.55
V_2O_5	1.4	1.55	0.65

In a view of above discussion the Ti-doped glass exhibited the most desirable PL band over the UV and violet region due to more condensed precipitation of small particle size of willemite and ZnO crystals.

5. Conclusion

ZnO crystals were the only crystalline phase of our base glass with the composition of $60ZnO–25SiO_2–15B_2O_3$. Adding 2 mole TiO_2 to the base glass led to the crystallization of ZnO particles, whereas adding 3 mole TiO_2 facilitated the crystallization of willemite in addition to ZnO crystals. Similarly V_2O_5 acted as a nucleating agent for willemite and vanadium oxide crystals in V-doped samples. On the other hand the visible band emitted from ZnO was eliminated in all studied samples as a result of embedding ZnO in a borosilicate glass matrix, since intrinsic defects such as oxygen vacancies are more limited in glasses. This together with the effect of Ti and V on the enhancement of both intensity and width of the near-band-edge peak is very desirable in scintillating applications. However, the presence of various peaks over the emitted band of the 3 mole V_2O_5 – doped glass due to the occurrence of different valencies in vanadium oxide is not approvable in scintillating glasses. Therefore, the Ti-doped glass is considered as the optimum composition from both viewpoints of microstructure and photoluminescence properties.

References

[1] L. Ding, Y. Yang, X. Jiang, C. Zhu, G. Chen, Photoluminescence of undoped and B-doped ZnO in silicate glasses, J. Non-cryst. Solids 354 (2008) 1382–1385.
[2] G. Qian, S. Baccaro, M. Falconieri, J. Bei, A. Cecilia, G. Chen, Photoluminescent properties and raman spectra of ZnO-based scintillating glasses, J. Non-Cryst. Solids 354 (2008) 4626–4629.
[3] D. Millers, L. Grigorjeva, W. Lojkowski, T. Strachowski, Luminescence of ZnO nanopowders, J. Radiat. Meas. 38 (2004) 589–591.
[4] Z. Fu, W. Dong, B. Yang, Z. Wang, Y. Wang, Effect of MgO on the enhancement of ultraviolet photoluminescence in ZnO, J. Solid State Commun. 138 (2006) 179–183.
[5] V.A. Dijken, E.A. Meulenkamp, D. Vanmaekelbergh, A. Meijerink, The luminescence of nanocrystalline ZnO particles: the mechanism of the ultraviolet and visible emission, J. Lumin. 87 (2000) 454–456.
[6] S. Zhao, Z. Ji, Y. Yang, D. Huo, Y. Lv, Nano-ZnO embedded SiO_2 glass with intense ultraviolet emission, J. Mater. Lett. 61 (2007) 2547–2550.
[7] A. Arora, A. Goel, E.R. Shaaban, K. Singh, O.P. Pandey, J.M.F. Ferreira, Crystallization kinetics of $BaO–ZnO–Al_2O_3–B_2O_3–SiO_2$ glass, J. Physica B 403 (2008) 1738–1746.
[8] J. Zhou, F. Zhao, Y. Wang, Y. Zhang, L. Yang, Size-controlled synthesis of ZnO nanoparticles and their photoluminescence properties, J. Lumin. 122–123 (2007) 195–197.

[9] L. Ding, Y. Yang, X. Jiang, C. Zhu, G. Chen, Photoluminescence of undoped and B-doped ZnO in silicate glasses, J. Non-Cryst. Solids 354 (2008) 1382–1385.
[10] M.B. Volf, Chemical Approach to Glass, Elsevier, Amsterdam, Oxford, Tokyo, New York, 1984.
[11] G. Qian, S. Baccaro, A. Guerra, L. Xiaoluan, Y. Shuanglong, G. Iurlaro, G. Chen, Gamma irradiation effects on ZnO-based scintillating glasses containing CeO_2 and/or TiO_2, J. Nucl. Instrum. Methods Phys. Res. B 262 (2007) 276–280.
[12] K.M. Lin, C.C. Lin, C.Y. Hsiao, Y.Y. Li, Synthesis of $Gd_2Ti_2O_7:Eu^{3+}$, V^{4+} phosphors by sol–gel process and its luminescent properties, J. Lumin. 127 (2007) 561–567.
[13] G. Chen, M. Nikl, N. Solovieva, A. Beitlerova, J. Rao, Y. Yanga, Y. Zhang, X. Jiang, C. Zhu, Photoluminescent properties of nanocrystallized zinc borosilicate glasses, J. Radiat. Meas. 38 (2004) 771–774.
[14] G. Qian, M. Nikl, J. Bei, J. Pejchal, S. Baccaro, R. Cecilia, G. Chen, A. Giorgi, Temperature dependence of photoluminescence in ZnO-containing glasses, J. Opt. Mater. 30 (2007) 91–94.
[15] S.E. Derenzo, M.J. Weber, E. Bourret-Courchesne, M.K. Klintenberg, The quest for the ideal inorganic scintillator, J. Nucl. Instrum. Methods Phys. Res. Sect. A 505 (2003) 111–117.
[16] J.A. Duffy, M.D. Ingram, Optical basicity—IV: Influence of electronegativity on the Lewis basicity and solvent properties of molten oxyanion salts and glasses, J. Inorg. Nucl. Chem. 37 (1975) 1203–1206.
[17] L. Pauling, The Nature of Chemical Bond, third ed., Cornell University Press, Ithaca, NewYork, 1960.
[18] E.S. Mostafa, The uncertainties of the calculated optical basicity from the optical band gap and the refractive index for some oxide glasses, J. Appl. Sci. 5 (10) (2005) 1867–1870.
[19] N. Tahir, S.T. Hussain, M. Usman, S.K. Hasanain, A. Mumtaz, Effect of vanadium doping on structural, magnetic and optical properties of ZnO nanoparticles, J. Appl. Surf. Sci. 255 (2009) 8506–8510.
[20] H. Singh, K. Singh, L. Gerward, K. Singh, H.S. Sahota, R. Nathuram, $ZnO–PbO–B_2O_3$ glasses as gamma-ray shielding materials, J. Nucl. Instrum. Methods Phys. Res. B 207 (2003) 257–262.
[21] J. Nie, J. Zhang, J. Bei, G. Chen, Optical properties of zinc barium silicate glasses, J. Non-Cryst. Solids 354 (2008) 1361–1364.